



We are Nitinol.™

**Characterization of the Aging Response of a Melt-Sun Al-Be-Li Alloy Ribbon**

Nieh, Pelton, Oliver, Wadsworth

Metallurgical Transactions

Vol. 19A

May 1988

pp. 1173-1178

1988

# Characterization of the Aging Response of a Melt-Spun Al-Be-Li Alloy Ribbon

T. G. NIEH, A. R. PELTON, W. C. OLIVER, and J. WADSWORTH

A rapidly solidified Al-10 wt pct Be-3 wt pct Li alloy has been produced by a melt-spinning technique. The aging behavior of the melt-spun ribbon has been characterized by a number of techniques, including differential scanning calorimetry, hardness measurements, and transmission electron microscopy. The results have shown that the aging responses of the ternary Al-Be-Li alloy are very similar to those of Al-Li binary alloys. Specifically,  $\delta'$  precipitates are formed at temperatures near 180 °C and they transform to  $\delta$  at temperatures around 300 °C. Microstructural examination indicates that, in the Al-Be-Li alloy,  $\alpha$ -Be particles are present in the matrix as independent dispersoids and, apparently, have little effect on the aging behavior of the Al-Li matrix; no new phases are present in the matrix of specimens heat treated up to 400 °C. The  $\alpha$ -Be particles coarsen, however, above a temperature of approximately 300 °C. The growth of  $\alpha$ -Be particles follows the classical Ostwald coarsening type of mechanism.

## I. INTRODUCTION

LITHIUM and beryllium are the only two elemental additions to aluminum that can simultaneously increase the elastic modulus and reduce the density in a significant manner. Al-Li alloys can be produced by powder metallurgy (PM), as well as ingot metallurgy (IM), because of the large solid solubility of Li in Al. In contrast, because of the limited solid solubility (about 0.1 pct by weight maximum) of Be in Al, fine-structured Al-Be based alloys containing high Be levels can be produced only by rapid solidification processing (RSP). Although binary Al-Be alloys have been under investigation during the last few years,<sup>[1]</sup> ternary Al-Be-Li alloys have not yet been extensively explored. In view of the potential weight savings of such low density alloys, as well as the improvements in elastic modulus, the Al-Be-Li system is an extremely attractive one that merits detailed study.

Recently, Wadsworth and co-workers<sup>[2-5]</sup> studied Al-Be-Li alloys produced by arc casting, splat quenching, and melt spinning techniques.<sup>[2]</sup> They found that in the as-spun condition, RSP Al ribbons containing both Li and Be contain two types of precipitates that form independently:  $\delta'$  ( $\text{Al}_3\text{Li}$ ) precipitates in the form of coherent spheroids whereas the  $\alpha$ -Be precipitates in the form of dispersoids. In addition, it was also observed that Li- and Be-rich oxide layers are easily formed on the surfaces of these RSP ribbons that have been subjected to an oxidation environment.<sup>[6]</sup>

It is generally believed that hydrogen is one of the major elements responsible for poor weldability of powder metallurgy materials, because it often generates voids or microvoids during fusion welding. Also, there is considerable evidence to suggest that the presence of hydrogen in Al is detrimental to its ductility.<sup>[7,8]</sup> It is useful, therefore, to conduct Thermal Analysis/Mass Spectroscopy (TA/MS) experi-

ments to determine the outgassing behavior of RSP ribbons. Such information can be incorporated into Al-Be-Li alloy processing schedules.

The main purpose of this study is to investigate the heat-treatment response of RSP Al-Be-Li ribbons. The microstructural evolution in the heat-treated ribbons was analyzed using a number of supplementary techniques, including Differential Scanning Calorimetry (DSC), conventional and nanoindentor hardness measurements, and Transmission Electron Microscopy (TEM).

## II. EXPERIMENTAL PROCEDURE

An Al-10 pct Be-3 pct Li (percentage by weight) ternary alloy was prepared by arc melting high purity ingot stock Al, high-purity, battery-grade Li, and electrolytic induction melted Be stock. The arc melted button was converted to melt spun ribbon of approximately 5 mm in width and less than 0.1 mm thickness using an apparatus and techniques described elsewhere.<sup>[2,3]</sup>

TA/MS analysis was carried out by placing alloy ribbons (0.05 g to 0.5 g) in a quartz container. Ultra-pure helium was allowed to sweep over the sample in a continuous fashion (20 to 40 ml/min at  $7 \times 10^4$  Pa gas pressure) so that any degassed species were transferred into a mass spectrometer via a heated (100 °C) thin walled stainless steel transfer line. The mass spectrometer continuously monitors the species which degas from the sample as the tube is heated from ambient to high temperature (600 °C herein) at a fixed rate (16 °C/min herein). A brief description of the experimental apparatus has been reported elsewhere.<sup>[9]</sup>

DSC testing was conducted in high purity helium gas with approximately 8 mg of comminuted ribbons. The test was carried out between room temperature and 550 °C. Both the heating and cooling rates were controlled to 20 °C/min. All test ribbons were encapsulated in a quartz tube and evacuated to approximately 1 Pa prior to heat treatment. This encapsulation was necessary to minimize the oxidation of the ribbon; oxidation could introduce artificial effects on the microstructure and on microhardness measurements. Heat treatment was conducted using either a silicone oil bath or an air furnace, depending on the temperature. Each

T. G. NIEH is Staff Scientist, Research and Development Division, Lockheed Missiles and Space Co., Inc., 3251 Hanover Street, Palo Alto, CA 94304. A. R. PELTON is Assistant Professor, Department of Materials Science and Engineering, University of Notre Dame, Notre Dame, IN 46556. W. C. OLIVER is Research Scientist, Metals and Ceramics Division, Oak Ridge National Laboratory, P.O. Box X, Oak Ridge, TN 37630. J. WADSWORTH is Manager, Metallurgy Department, Research and Development Division, Lockheed Missiles and Space Co., Inc., Palo Alto, CA 94304.

Manuscript submitted May 6, 1987.

heat treated sample was sectioned into two, one for TEM examination and the other metallographically mounted for hardness measurements.

Specimens for TEM were hand ground to approximately 30  $\mu\text{m}$  thick and then mounted on 3 mm mounting rings with epoxy. These samples were dual-ion milled with  $\text{Ar}^+$  at 4 kV and a 30  $\mu\text{A}$  specimen current. This procedure, although time consuming, produced somewhat better specimens than those produced by electrochemical methods. In particular, electrothinning tends to etch out  $\alpha$ -Be particles.

All metallographic specimens were cold-mounted and final polished with a 0.1  $\mu\text{m}$  CeO compound prior to the hardness measurements. Two different techniques were used to obtain the hardness values from these specimens. One technique utilized a conventional Leitz miniloading microhardness machine (MH), but a much smaller load (4.043 g) was applied than is normally used (>25 g). The instrument was calibrated immediately before the tests. The actual area of contact between the indent and the test specimen was measured using a high resolution optical microscope. The typical size of an indent was approximately 7  $\mu\text{m}$ . It is expected that an inherent error of approximately 7 to 15 pct may result from determining the exact size of an indent; this error may result in a 15 to 30 pct scatter in hardness values. The other method was to use a nanoindenter or Mechanical Property Microprobe (MPM). This technique uses a well-controlled diamond indent head to penetrate into the test specimen. The hardness value was calculated from the load vs depth curve. The MPM test is primarily a dynamic method. The typical size of an indent was roughly 3  $\mu\text{m}$  for a 500 nm penetration depth. Details of the test apparatus, as well as the test procedures, have been given elsewhere.<sup>[10]</sup> It is noted that the sizes of indent for both hardness tests are small compared to the thickness (about 20 times) of the ribbons, thus avoiding edge effects.

### III. RESULTS AND DISCUSSION

#### A. Thermal Analysis and Mass Spectroscopy (TA/MS)

The TA/MS analysis indicates that the ribbons were relatively clean. The only significant degassed species was hydrogen, which evolves at approximately 350 to 470  $^{\circ}\text{C}$  during heating analysis. Oxide dehydration, which normally takes place for other Al powders at about 120  $^{\circ}\text{C}$ ,<sup>[11]</sup> was not observed in this study. This difference in behavior may be directly related to the surface oxide states of the ribbon. For conventional Al alloy powders, the surface oxide is either  $\text{Al}_2\text{O}_3$  or an  $\text{Al}_2\text{O}_3$ -MgO mixture; the surface oxide on Al-Be-Li powders is primarily  $\text{Li}_2\text{O}$ .<sup>[3]</sup> Different oxides would be expected to have different physisorption characteristics for water. From the TA/MS data, it is concluded that a minimum temperature of about 400  $^{\circ}\text{C}$  is needed for removal of residual hydrogen from the as-spun ribbons prior to consolidation.

#### B. Differential Scanning Calorimetry (DSC)

The result of a DSC test is shown in Figure 1, in which a DSC curve from the as-spun Al-Be-Li ribbon is shown from room temperature to about 550  $^{\circ}\text{C}$ . Three major reactions, occurring at approximately 180, 300, and 400  $^{\circ}\text{C}$ , are readily observed on this DSC curve. It has been pointed

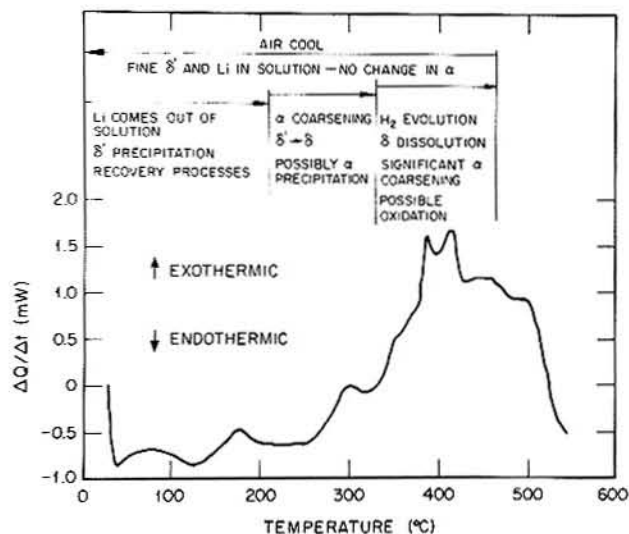


Fig. 1—Data from a differential scanning calorimetry trace from the as-spun Al-10 pct Be-3 pct Li ribbon (at 20 K/min).

out by Kissinger<sup>[12]</sup> and Louis and Garcia-Cordovilla<sup>[13]</sup> that the maximum reaction rate corresponds to the peak of the DSC curve. The as-spun ribbon is essentially in the solution treated condition. The first exotherm at 170 to 180  $^{\circ}\text{C}$  is believed to be due to a uniform  $\delta'$  ( $\text{Al}_3\text{Li}$ ) precipitation. The next exotherm, recorded at 290 to 300  $^{\circ}\text{C}$ , is due to the  $\delta'$  to  $\delta(\text{AlLi})$  transformation. The last exotherm, however, which takes place at a temperature around 400  $^{\circ}\text{C}$ , is somewhat more difficult to explain. To understand this exotherm, transmission electron microscopy was conducted using an Al-Be-Li ribbon that had been thermally exposed at 405  $^{\circ}\text{C}$  for 30 minutes.

As shown in Figure 2, there are only three precipitate phases that can be identified in the microstructure; these are  $\alpha$ -Be,  $\delta'$ , and  $\delta$ . It should be noted that the average size (280 nm) of the  $\alpha$ -Be particles after 400  $^{\circ}\text{C}$  exposure is much larger than that found in the as-spun condition (140 nm). In addition to coarsening of the  $\alpha$ -Be particles, it is also found that there is a large amount of  $\delta'$  phase



Fig. 2—Microstructure of an RSP Al-10 pct Be-3 pct Li ribbon heat treated at 405  $^{\circ}\text{C}$  for 0.5 h. There are three precipitate phases present in the matrix:  $\alpha$ -Be,  $\delta'$ , and  $\delta$ .

in the matrix. The presence of  $\delta'$  is apparently due to reprecipitation upon cooling from the heat treat temperature of 405 °C. The  $\delta'$  reprecipitation can, however, only take place on cooling (not on heating) of the ribbons and, therefore, cannot contribute to the DSC curve shown in Figure 1. This result is similar to that found in Al-Li alloys by Baumann and Williams.<sup>[14]</sup> Papazian *et al.*<sup>[15]</sup> have also reported that dissolution of  $\delta$  may take place at temperatures near 400 °C. In summary, the coarsening of  $\alpha$ -Be particles and dissolution of  $\delta$  are taking place simultaneously at this temperature. Although the former reaction is exothermic, the later one is endothermic. Therefore, the DSC curve for the 400 °C peak actually represents a summation of the above concurrent events. Although the TEM study shows evidence for the two processes, it is difficult to evaluate, quantitatively, the relative contribution from each of them.

Since Al, Be, and Li are all strong oxide formers, oxidation of the ribbons may still occur during the DSC experiment, despite the use of high purity helium environments during heating. Oxidation of the ribbons is expected to have a significant effect on the final DSC analysis. A special effort was subsequently made using Auger Electron Spectroscopy to examine the surface chemistry, as well as the oxide thicknesses, of ribbons that had been heat treated under a simulated condition for a DSC test. The experimental results failed to show any significant difference between the ribbon that had been subjected to such a simulation and the as-spun ribbon.

In summary, the DSC experiment suggests that the presence of Be has essentially no direct effect on the aging behavior in the Al-Li alloy matrix. The aging characteristics for the Al-Be-Li ternary alloy were virtually identical to an Al-Li binary alloy. There is no chemical or metallurgical interaction between Al and Be, or between Li and Be.

### C. Hardness Measurements

Hardness data were measured at room temperature from ribbons that had been heat treated at various temperatures for 1 hour. These data are summarized in Figure 3; each datum point in the figure represents an average value from at least five measurements. The hardness value of the as-spun ribbon is 2.3 GPa and remains essentially constant after heat treatment at temperatures below 150 °C but then starts to decrease to a value of 1.5 GPa after heat treatment at temperatures from 165 to 185 °C. After heat treatment at temperatures above 185 °C, the room temperature hardness rises and reaches a peak of 1.9 GPa (after heat treatment at 210 °C) and then drops to 1.5 GPa (after heat treatment at 250 °C). As the temperature of heat treatment further increases, the hardness slowly decreases. The lowest hardness value measured was 1.0 GPa, after heat treatment at 500 °C.

The first decrease in hardness in Figure 3 is believed to be mainly due to dislocation annihilation in the as-spun ribbon. It has previously been shown that in the as-spun condition, these alloys normally contain a large number of dislocations.<sup>[4]</sup> At heat treatment temperatures of about 180 °C,  $\delta'$  precipitates form rapidly which causes hardening of the alloy. Apparently, this hardening effect is nullified by the softening that results from dislocation annihilation. The hardness peak that takes place at 210 °C was somewhat unexpected. In order to understand the ef-

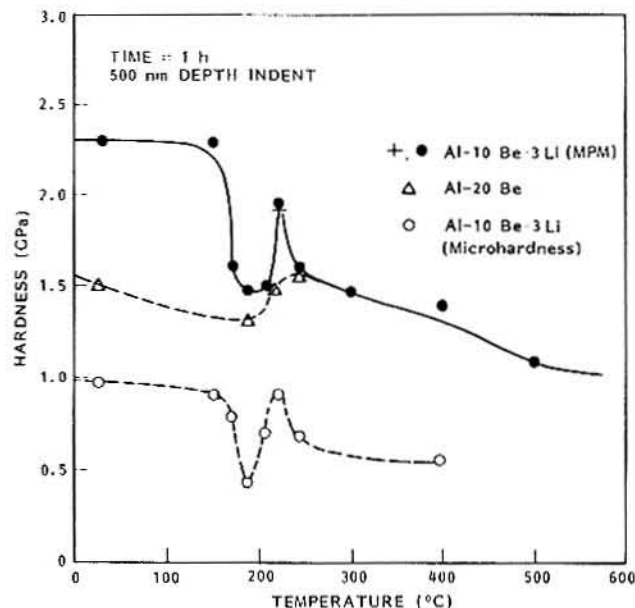


Fig. 3—Hardness values as a function of heat-treat temperature for Al-10 pct Be-3 pct Li and Al-20 pct Be ribbons. The hardness measurements were obtained from both MPM and conventional microhardness tests.

fect of Be on the overall aging characteristics in these Al-Be-Li alloys, RSP ribbons of binary Al-20 pct Be alloy were also prepared and their aging behavior was studied.

The hardness values measured from the heat treated binary Al-Be ribbons are also included in Figure 3. The initial hardness (1.5 GPa) is much lower than in the Al-Be-Li alloys. After annealing at 185 °C, it drops to a value of 1.3 GPa. In the heat treatment range of 210 to 240 °C, however, the hardness increases to 1.6 GPa. It is important to note that in this respect the binary alloy ribbons and the ternary alloy ribbons exhibit aging peaks at almost the same temperature range, strongly suggesting that the aging peak is probably due to precipitation of Be particles alone. The precipitation of Be particles from supersaturated solid solutions (the maximum equilibrium solid solubility for Be in Al is about 0.3 at. pct or 0.1 wt pct at 645 °C) in RSP Al-Be-Li and Al-Be ribbons, apparently takes place at temperatures near 200 °C, and results in a hardness increase. Microstructural evidence for the reprecipitation of Be particles was difficult to obtain from the TEM examination, due to the large amount of Be particles already present in the as-spun specimens. It is noted that this aging peak has not been previously observed in consolidated and extruded Al-Be-Li alloys.<sup>[12]</sup> This is probably because the precipitation that leads to hardening is an irreversible reaction and the consolidation technique used to fabricate bulk Al-Be-Li alloys from melt-spun ribbon had already triggered the reaction. A possible explanation for the absence of evidence for this precipitation in the DSC results is that either (1) the heat of enthalpy of the reaction is too low or (2) the fine, secondary, precipitates were quickly consumed by coarsening of the primary  $\alpha$ -Be particles.

At aging temperatures of above 300 °C, the  $\delta'$  precipitate transforms entirely into  $\delta$  phase and the  $\alpha$ -Be particles also start to coarsen rapidly. Both events, together with grain growth, result in a decrease in hardness. The microstructural evidence for the  $\delta'$  to  $\delta$  transformation, as well as the

$\alpha$ -Be particle coarsening behavior at 300 °C, is presented in the next section.

Microhardness measurements using a conventional microhardness testing machine were also made using metallographically mounted specimens. Ten measurements were taken from each specimen. The average hardness values, as a function of annealing temperature, are plotted in Figure 3. Despite the significant differences in the operational principles, the general trend of the hardness data is similar for the MPM test and the MH test. The absolute hardness values from the MH test are, however, lower than those from the MPM test. This is consistent with some classical observations,<sup>[16]</sup> namely, the hardness value decreases as the indent size increases.

#### D. Microstructure Examination

A transmission electron micrograph is shown in Figure 4 of the microstructure of an as-spun ribbon of Al-10 pct Be-3 pct Li. Both the  $\alpha$ -Be particles and  $\delta'$  precipitates are readily observed in the microstructure. The Be particles, in general, exhibit a smooth morphology and do not show any preferential orientation with respect to the matrix. Although the  $\alpha$ -Be particles in this figure appear to be of uniform size, they in fact range from 65 to 120 nm. A large number of quenched-in dislocations are also found in the microstructure.

By contrast, after aging at 185 °C, the dislocation density is drastically reduced, as shown in Figure 5. This dislocation reduction is reflected in the decrease of hardness values (Figure 3). The size distribution of the  $\alpha$ -Be particles appears, however, similar to that in the as-spun condition. The dark-field microstructure (using the  $\langle 100 \rangle$   $\delta'$  superlattice reflection to show the  $\delta'$  precipitate distribution) from the same area in Figure 5 is illustrated in Figure 6. It is evident that the  $\delta'$  precipitates are uniformly distributed throughout the grain interior. It is noted that 185 °C is the isothermal, peak-aging temperature for both Al-Li and Al-Be-Li alloys.<sup>[12,17]</sup> Heat treatment of the ribbon at temperatures higher than 185 °C results in overaging, and the  $\delta'$  precipitates gradually transform to  $\delta$  precipitates. This transformation is illustrated in Figure 7, which shows the microstructure of an Al-10 pct Be-3 pct Li RSP ribbon heat

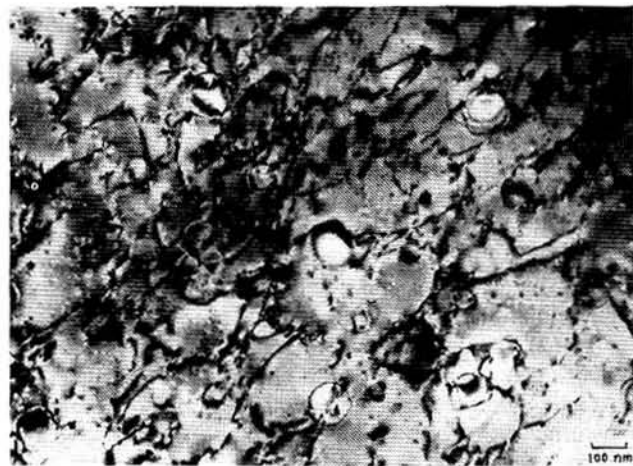


Fig. 4—Microstructure of an as-spun Al-10 pct Be-3 pct Li ribbon. Both the  $\alpha$ -Be particles and  $\delta'$  precipitates are visible.



Fig. 5—Microstructure of RSP Al-10 pct Be-3 pct Li ribbon heat-treated at 185 °C for 1 h.

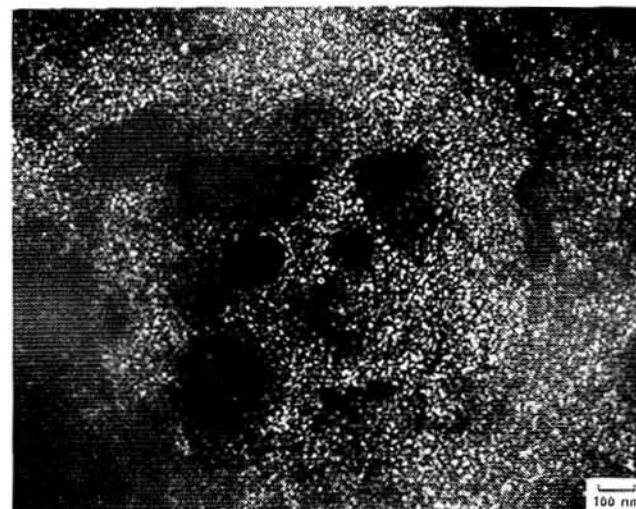


Fig. 6—Corresponding dark-field photomicrograph from the area illustrated in Fig. 5; the uniform distribution of  $\delta'$  is illustrated.

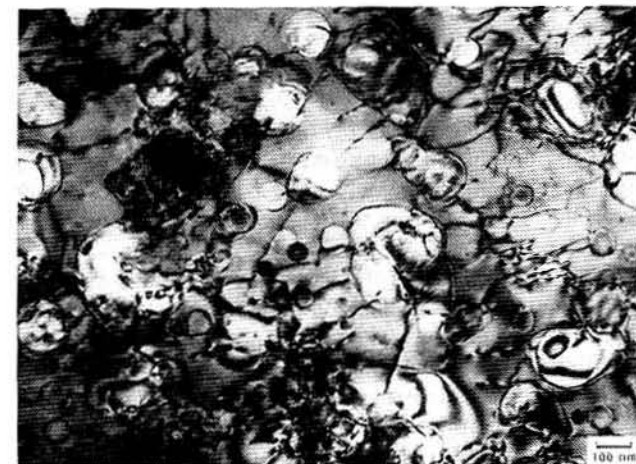


Fig. 7—Microstructure of an RSP Al-10 pct Be-3 pct Li ribbon heat-treated at 300 °C for 24 h. Selected area diffraction analysis does not show any  $\delta'$  precipitate in the matrix.

treated at 300 °C for 24 hours. Selected area diffraction from such a ribbon does not show any  $\delta'$  reflection. This suggests that all  $\delta'$  precipitates present in the original RSP ribbon have already been transformed into  $\delta$  precipitates. Heat treatment of the ribbon to temperatures higher than 300 °C causes some of the  $\delta$  precipitates to dissolve and  $\delta'$  to re-precipitate during cooling. This phenomenon was discussed and shown earlier in Figure 2.

An attempt was made to measure the average sizes of the  $\alpha$ -Be particles as a function of heat treatment temperature. Data from statistical measurements are presented in Figure 8. As shown in the figure, the size distribution for  $\alpha$ -Be particles is, in general, not very uniform. This causes a relatively large scatter in the size determination. Despite the large scatter, the data indicate that Be particles coarsen significantly at temperatures above 250 °C. Below 250 °C, the average particle sizes are rather close; variations about the average size are within the scatter band. This observation of Be particles coarsening is consistent with the hardness measurements.

Measurements of the coarsening rate of  $\alpha$ -Be particles at 300 °C were also carried out. The results are shown in Figure 9. In the figure, the average  $\alpha$ -Be particle size is plotted as a function of  $t^{1/3}$ , where  $t$  is the annealing time. The particle size appears to be proportional to  $t^{1/3}$ , suggesting a bulk diffusion controlled growth mechanism;<sup>[18]</sup> *i.e.*, particle growth by classical Ostwald ripening.

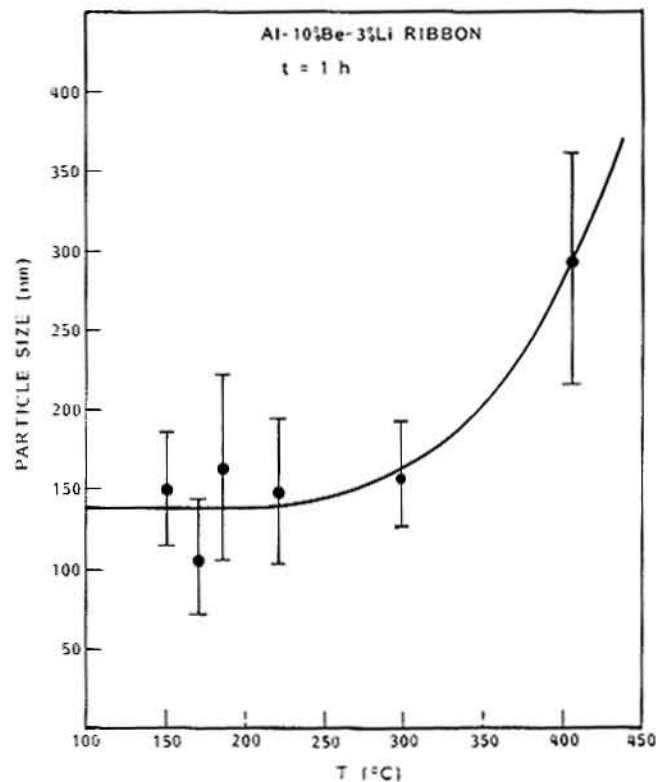


Fig. 8—Particle size of  $\alpha$ -Be as a function of heat treatment temperature. Particle coarsening appears to take place at temperatures of about 250 to 300 °C.

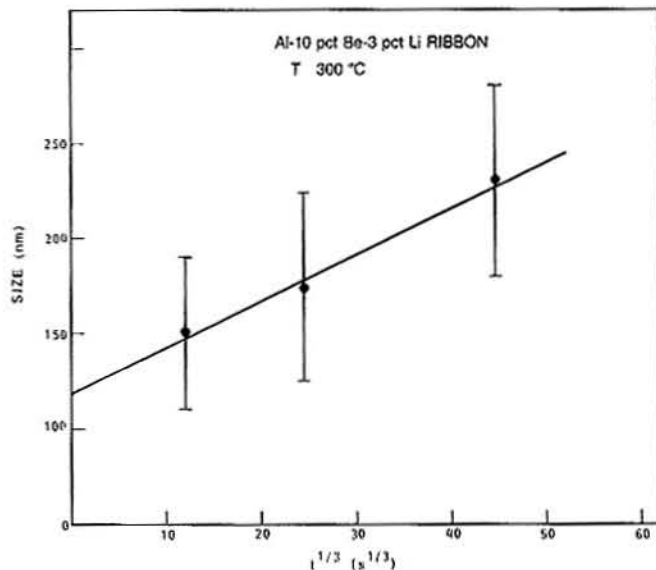


Fig. 9—Particle diameter of  $\alpha$ -Be as a function of  $t^{1/3}$ , where  $t$  is the annealing time. The linearity of the plot suggests that the coarsening behavior can be described by classical Ostwald ripening.

#### IV. CONCLUSIONS

The aging behavior of rapidly solidified Al-10 pct Be-3 pct Li ribbons and Al-20 pct Be ribbons has been characterized. The conclusions from this study are as follows:

1. The general aging characteristics of ternary RSP Al-Be-Li alloys are very similar to binary RSP Al-Li alloys.
2. Although  $\delta'$  precipitates are present in the as-spun ribbon, uniform  $\delta'$  distribution was not observed until aging at about 180 °C. Heat treatment of the ribbon at high temperatures, *e.g.*, 300 °C, resulted in the  $\delta'$  to  $\delta$  transformation.
3. In the Al-Be-Li ternary, the  $\alpha$ -Be particles are present in the Al-Li matrix as independent dispersoids and have little effect on the aging response of the Al-Li matrix. However,  $\alpha$ -Be does precipitate out from an extended Al-Be solid solution at a temperature of approximately 210 °C.
4. The size distribution of the  $\alpha$ -Be particles is not uniform. Upon heat treatment at temperatures greater than 250 °C,  $\alpha$ -Be particles coarsen and the growth behavior of these particles follows a classical Ostwald coarsening mechanism.

#### ACKNOWLEDGMENTS

The authors would like to thank Messrs. J. T. Allen and D. D. Crooks for carrying out some of the mechanical tests and manufacturing the alloy ribbons. This work was in part supported by the Office of Naval Research under Contract N00014-84-C-0032 and in part by the Division of Materials Science, United States Department of Energy under contract DE-AC05-84OR21400 with Martin Marietta Energy Systems, Inc.

## REFERENCES

1. R. E. Lewis: Progress Report for June-Sept. 1985, Naval Air Development Contract No. N62269-84-C-036.
2. A. E. Vidoz, D. D. Crooks, R. E. Lewis, I. G. Palmer, and J. Wadsworth: *Rapidly Solidified Powder Aluminum Alloys*. M. E. Fine and E. A. Starke, eds., ASTM STP No. 890, Amer. Soc. for Testing of Materials, Philadelphia, PA, 1986.
3. J. Wadsworth, A. Joshi, D. D. Crooks, and A. E. Vidoz: *J. Mater. Sci.*, 1986, vol. 21, pp. 3843-49.
4. J. Wadsworth, A. R. Pelton, D. D. Crooks, R. E. Lewis, and A. E. Vidoz: *J. Mater. Sci.*, 1986, vol. 21, pp. 3850-58.
5. J. Wadsworth, A. R. Pelton, and A. E. Vidoz: *Int. Jour. Mater. Sci. Eng.*, 1986, vol. 80, pp. L23-L26.
6. A. Joshi, J. Wadsworth, and A. E. Vidoz: *Scripta Metall.*, 1986, vol. 20, pp. 529-32.
7. R. J. Gest and A. R. Troiano: *Corrosion*, 1974, vol. 30, (8), pp. 274-79.
8. D. P. Hill and D. N. Williams: Final Report, Contract No. N00019-81-C-0433, Oct. 1982.
9. J. G. Moncur, A. B. Campa, and P. C. Pinoli: *J. High Resolution Chromotography*, 1982, vol. 5, pp. 322-24.
10. J. B. Pethica, R. Hutchings, and W. C. Oliver: *Phil. Mag.*, 1983, vol. 48A, (4), pp. 593-606.
11. *Proc. 3rd Conf. on Rapid Solidification Processing*, R. Mehrabian, ed., National Bureau of Standards, Gaithersburg, MD, Dec. 1982, p. 521.
12. H. E. Kissinger: *Anal. Chem.*, 1957, vol. 29, pp. 1702-17.
13. E. Louis and C. Garcia-Cordovilla: *J. Mater. Sci. Lett.*, 1984, vol. 19, p. 689.
14. S. F. Baumann and D. B. Williams: *Aluminum-Lithium II*. E. A. Starke, Jr. and T. H. Sanders, Jr., eds., TMS-AIME, Warrendale, PA, 1984, p. 17.
15. J. M. Papazian, C. Sigli, and J. M. Sanchez: *Scripta Metall.*, 1986, vol. 20, pp. 201-06.
16. R. A. Oriani: *Acta Metall.*, 1964, vol. 12, pp. 1399-1409.
17. D. B. Williams: *Aluminum-Lithium Alloys*, T. H. Sanders, Jr. and E. A. Starke, Jr., eds., TMS-AIME, Warrendale, PA, 1981, pp. 89-100.
18. I. M. Lifshitz and V. V. Slyozov: *J. Phys. Chem. Solids*, 1961, vol. 19, p. 35.